Pramana – J. Phys., Vol. 38, No. 4, April 1992, pp. 397–409. © Printed in India.

Characterization of supersonic beams by time-of-flight technique

P N BAJAJ and P K CHAKRABORTI
MDRS, Bhabha Atomic Research Centre, Bombay 400085, India

MS received 20 August 1991

Abstract. Time-of-flight technique has been used to characterize supersonic beams of polyatomic molecules in terms of translational and vibrational temperatures, various velocity parameters and speed ratio. Collision effectiveness and effective specific heat ratio of polyatomic gases pertinent to jet expansion have also been determined and interpreted.

Keywords. Nozzle beam; time-of-flight technique.

PACS Nos 34·50; 82·20

1. Introduction

Supersonic free-jets and supersonic beams produced therefrom possess many special characteristics, such as high degree of directionality, high beam intensity, narrow velocity distribution, low internal temperatures for polyatomic molecules, orientation of the reagents, nearly collision-free environment and state selection. These attractive features have led to their extensive use in a variety of fields, e.g., spectroscopy (Levy 1980; Shea and Flygare 1982; Travis *et al* 1977; Gough *et al* 1977; Vallentini *et al* 1980; Snavely *et al* 1981), isotope separation (Amirav and Even 1980), chemical dynamics (King and Herschbach 1977; Stolte 1982; Schulz *et al* 1980), surface science studies (Cardillo *et al* 1978), condensation (Veeken and Reuss 1984; Valente and Bartell 1984; Miller *et al* 1984; Bajaj *et al* 1989), analytical chemistry (Hayes and Small 1983). Translational and internal temperatures decrease in a supersonic expansion as a result of elastic and inelastic collisions, which ultimately come to a halt due to rarefaction (Anderson and Fenn 1967). The exact frozen location of any degree of freedom depends upon its relaxation efficiency and the stagnation conditions. Thus, most of the beam properties depend strongly on the choice of source parameters, such as stagnation pressure, temperature, nozzle shape and diameter. On the other hand, a majority of molecular beam experiments demand a detailed knowledge of the beam characteristics. Thus, the study of supersonic molecular beams, in itself, is of great importance.

In this paper, we shall discuss and demonstrate the importance of the time-of-flight technique in characterization of supersonic beams in terms of various thermodynamic and gas kinetic parameters.

2. Experimental

The schematic of the experimental set-up is shown in figure 1. It consists of a differentially pumped two-chamber vacuum system, a nozzle-skimmer assembly, a

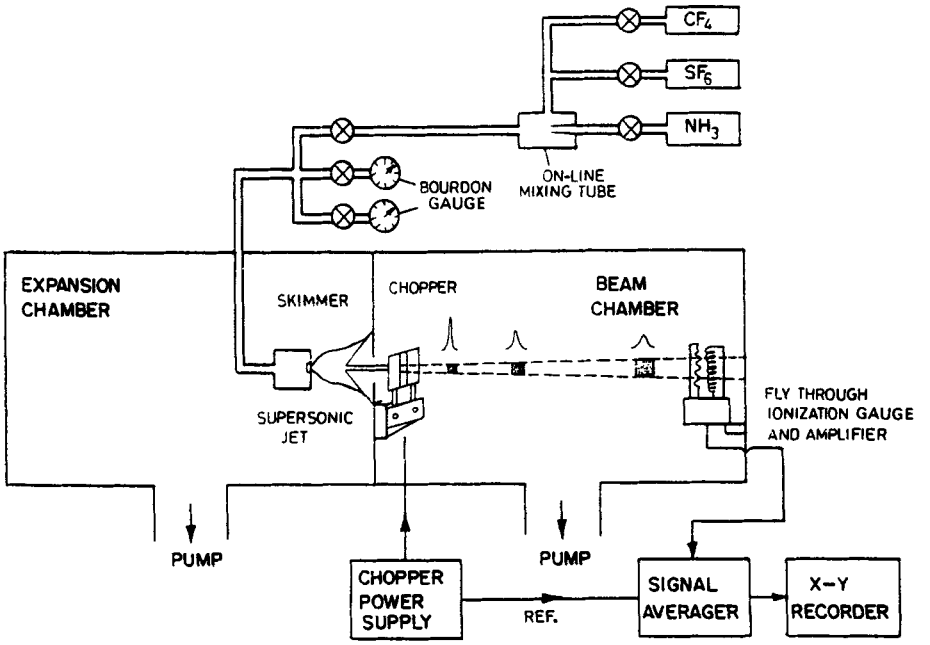

Figure 1. Schematic of the time-of-flight experimental set-up.

gas feeding and monitoring system, a tuning fork chopper, a beam flag, a fly-through ionization gauge and a signal averager (Nicolet-1170). The expansion chamber was pumped by a 9″ dia. LN_2 trapped diffusion pump backed by a 1200 litre min^{-1} rotrary pump, whereas the beam chamber was pumped by a 9″ dia. LN_2 trapped diffussion pump coupled to a 750 litre min^{-1} rotary pump. All the components of the system exposed to the high vacuum were fabricated out of S.S.-304. The pressures in the chambers were monitored by BA ionization gauges (CVC Products, Inc. Model GIC-300 A). In the absence of gas load, the typical pressure in the expansion chamber was 4×10^{-6} torr, and that in the beam chamber was 3×10^{-7} torr.

Molecular beam of the gas under study was generated by expanding the gas through a 75 μm dia. nozzle, and skimming the free-jet at the desired location. The collimated beam was chopped by a pulse type tuning fork chopper (Bulova, American Time Products), having a symmetric triangular gate function (fwhm = 100 μs), measured with a He–Ne laser and a photodiode. The delay between the trigger pulse from the power supply of the tuning fork chopper and the peak of the laser pulse was measured, and taken into account in the analysis of the data. The fly-through ionization gauge, (Beam Dynamics, Model *fig-* 1), having sensitivity of 1×10^5 V $torr^{-1} mA^{-1}$, mounted on the end-flange in the beam chamber at a distance of 41·5 cm from the chopper (cf. figure 1), was used to detect particle pulses. The output of the ionization gauge was amplified by a preamplifier, and processed by the signal averager. For determining the relative beam intensities, the emission current of the gauge filament was kept fixed at 1·2 mA throughout the investigation.

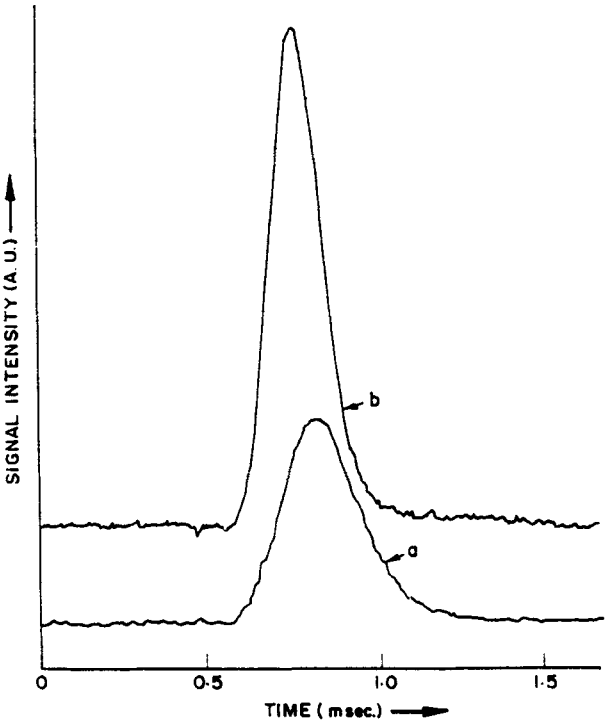

Figure 2. Experimental time-of-flight profiles of CHF_3 at two stagnation pressures. (**a**) $P_0 = 80$ torr; (**b**) $P_0 = 820$ torr.

3. Results and discussion

3.1 *Translation relaxation*

Typical time-of-flight (TOF) profiles of pure CHF_3 beams are shown in figure 2 for two different stagnation pressures. It is to be noted from the figure that pulse flight time corresponding to higher stagnation pressure is lower and the corresponding TOF profile is sharper than that at the lower pressure. This implies higher flow velocity and lower temperature at higher stagnation pressure. Quantitative analysis of a TOF profile to determine various beam parameters was carried out as follows. The number density-velocity distribution function for supersonic beams is (Anderson and Fenn 1967; Coulter *et al* 1980):

$$n(v_\parallel)\mathrm{d}v_\parallel = N_s \frac{v_\parallel^2}{\alpha_s^3} \exp\{-(v_\parallel - u)^2/\alpha_s^2\}\,\mathrm{d}v_\parallel \tag{1}$$

where u and α_s are flow velocity and characteristic velocity respectively. The normalization constant, N_s, is

$$N_s^{-1} = \frac{1}{4}[\pi^{1/2}(1 + 2S_\parallel^2)\{1 + \mathrm{erf}(S_\parallel)\} + 2S_\parallel \exp(-S_\parallel^2)]. \tag{2}$$

For $S > 4$,

$$N_s^{-1} = \frac{1}{2}\pi^{1/2}(1 + 2S_\parallel^2). \tag{3}$$

The velocity parameters such as the most probable velocity of the beam molecules, v_m, the average velocity, $\langle v_\parallel \rangle$, and the root mean square velocity, $\langle v_\parallel^2 \rangle^{1/2}$, required to determine the kinetic energy of the beam molecules, can be expressed as

$$v_m = \frac{1}{2}[u + \{u^2 + 6\alpha_s^2\}^{1/2}] \tag{4}$$

$$\langle v_\perp \rangle = N_s \pi^{1/2}\left[(1 + \mathrm{erf}(S_\parallel))\left\{\frac{1}{2}S_\parallel^2 u + \frac{3}{4}u\right\} + \frac{1}{2}(S_\parallel u + \alpha_s)\exp(-S_\parallel^2)\right] \tag{5}$$

$$\langle v_\parallel^2 \rangle^{1/2} = N_s^{1/2}\pi^{1/4}\left[\{1 + \mathrm{erf}(S_\parallel)\}\left\{\frac{1}{2}u^2 S_\parallel^2 + \frac{3}{2}u^2 + \frac{3}{8}\alpha_s^2\right\} + \left\{\frac{1}{2}S_\parallel u^2 + \frac{5}{4}u\alpha_s\right\}\exp(-S_\parallel^2)\right]^{1/2}. \tag{6}$$

For $S_\parallel > 4$, (5) and (6) reduce to

$$\langle v_\parallel \rangle = N_s \pi^{1/2}\left[uS_\parallel^2 + \frac{3}{2}u\right] \tag{7}$$

$$\langle v_\parallel^2 \rangle^{1/2} = N_s^{1/2}\pi^{1/4}\left[u^2 S_\parallel^2 + 3u^2 + \frac{3}{4}\alpha_s^2\right]^{1/2}. \tag{8}$$

The signal profile registered by a fast detector in a time-of-flight experiment using a δ-function chopper can be obtained by transforming (1) into time domain (Anderson and Fenn 1967)

$$g_{\mathrm{den}}^0(t) = \kappa t^{-4}\exp\{-(L/t - u)^2/\alpha_s^2\} \tag{9}$$

where κ is a constant and L is the flight distance.

In practice, however, any chopper used generally has a finite opening time. The signal registered by a fast detector would, therefore, be convolution of the flight time distribution, $g_{\mathrm{den}}^0(t)$ and chopper opening function, $g_s(t)$

$$I^+(L;t) = \int_0^t g_{\mathrm{den}}^0[L;t - t')]g_s(t')\mathrm{d}t'. \tag{10}$$

The detector and the associated electronics also have a finite rise time. Therefore, the measured signal profile is given by

$$I_{\mathrm{obs}}^+(L;t) = \int_0^t I^+[L;t - t']g_d(t')\mathrm{d}t' \tag{11}$$

where $g_d(t)$ is the detector response function. Symmetric triangular chopper function

can be expressed as

$$g_s(t) = \frac{g_s^0}{w} t \qquad \text{for } 0 \leqslant t \leqslant w \tag{12a}$$

$$g_s(t) = \frac{g_s^0}{w}(2w - t) \qquad \text{for } w \leqslant t \leqslant 2w \tag{12b}$$

$$g_s(t) = 0 \qquad \text{for } t \gg 2w \tag{12c}$$

where w is fwhm and g_s^0 is maximum open area of the chopper. The detector response function is given by (Alcalay and Knuth 1969; Young 1973).

$$g_d(t) = \frac{1}{\tau_d} \exp(-t/\tau_d) \tag{13}$$

where τ_d is the response time of the detector and the associated electronics.

The experimentally observed signal profile can be fitted to the two-parameter number density function, (11), to determine flow velocity, u, and characteristic velocity, α_s. The starting values of u and α_s were determined using the procedure of Bajaj and Chakraborti (1986). Figure 3 shows simulated and experimental spectra for CHF_3 ($P_0 = 320$ torr). From the fitted values of u and α_s, and speed ratio, S_∞, and translational temperature, T_∞, were determined as

$$S_\infty = \left(\frac{1}{2} mu^2/kT_\infty\right)^{1/2} = u/\alpha_s \tag{14}$$

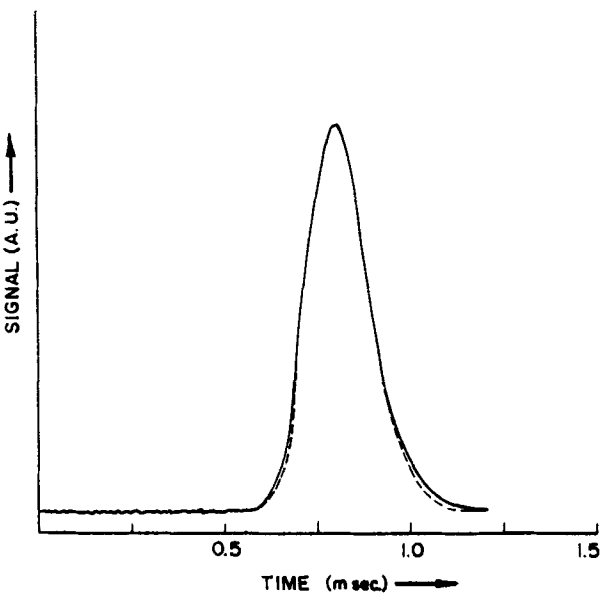

Figure 3. Experimental and simulated TOF profiles of CHF_3 ($P_0 = 320$ Torr) at a distance of 11·5 mm from the nozzle exit. Continuous curve is the experimental curve and dotted curve is the simulated profile.

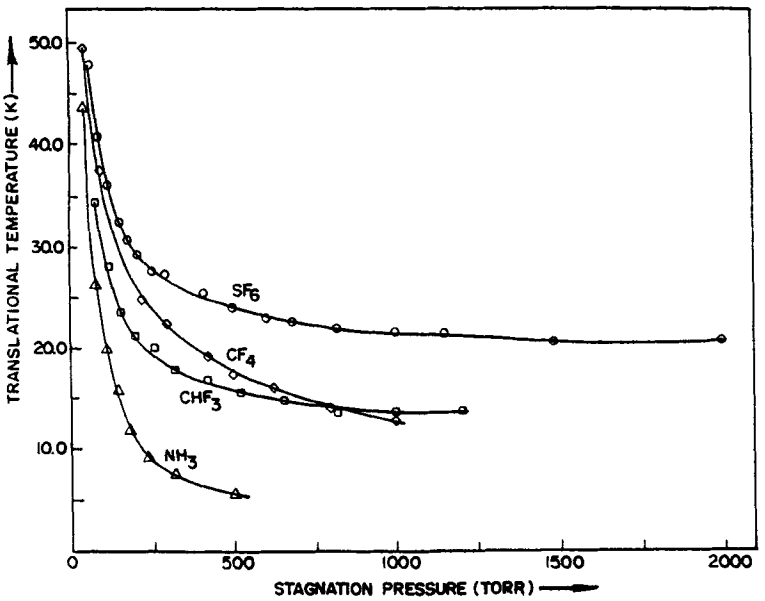

Figure 4. Translational temperature of various beam molecules at $X = 11{\cdot}5$ mm from the nozzle exit as a function of stagnation pressure.

and

$$T_{\parallel} = \alpha_s^2 (m/2k). \tag{15}$$

Once u and α_s are known, the most probable velocity, the average velocity and root mean square velocity can be determined from (4), (5) and (6) respectively.

The variation of the translational temperature of the beam with stagnation pressure is depicted in figure 4 for different gases. Translational temperature decreases with stagnation pressure for all the gases in the respective pressure ranges investigated, indicating increase in the degree of translational relaxation. Of the two spherical top molecules CF_4 and SF_6, the former attains lower temperature throughout the stagnation pressure range investigated, though it has lower hard-sphere collision cross-section (69·4 Å^2) as compared to that of the latter (95·4 Å^2). This may be attributed to lower degree of internal relaxation in CF_4 than that in SF_6. The observed effective specific heat ratio in supersonic expansion supports this interpretation (cf. § 3.3).

A more satisfactory way of assigning a temperature to a beam is to use the concept of mean kinetic energy within the beam (Brusdeylins *et al* 1976)

$$\frac{1}{2} k T_{\parallel} = \frac{1}{2} m \int_0^{\infty} (v_{\parallel} - u)^2 n(v_{\parallel}) \mathrm{d}v_{\parallel} \tag{16a}$$

$$= N_s \frac{m}{8} \left[u\alpha_s \exp(-S_{\parallel}^2) + \frac{\sqrt{\pi}}{2} (3\alpha_s^2 + 2u^2) \right]. \tag{16b}$$

For $S_{\parallel} > 8$

$$T_{\parallel} = \frac{m\alpha_s^2}{2k} \left[1 + \frac{2}{1 + 2S_{\parallel}^2} \right]. \tag{17}$$

In most of the cases, the values of $T_{\parallel}$ determined from (16) were higher than those determined from (15) by about 3%.

Tables 1–4 show flow velocity, u, characteristic velocity, α_s, the most probable velocity, v_m, average velocity, $\langle v_{\parallel} \rangle$, root mean square velocity, $\langle v_{\parallel}^2 \rangle^{1/2}$, and speed ratio, $S_{\parallel}$, of beams of the various gases, attained at a distance of 11·5 mm from

Table 1. Beam parameters of SF_6.

P_0 (Torr)	u (ms^{-1})	α_s (ms^{-1})	v_m (ms^{-1})	$\langle v_{\parallel} \rangle$ (ms^{-1})	$\langle v_{\parallel}^2 \rangle^{1/2}$ (ms^{-1})	$S_{\parallel}$
55	335·8	73·84	363·7	351·7	355·3	4·55
85	342·6	68·23	366·0	355·9	359·1	5·02
100	348·5	65·94	369·9	360·7	363·6	5·28
120	349·0	64·28	370·5	361·3	264·4	5·42
160	355·5	60·82	373·2	365·8	368·2	5·84
210	360·3	57·75	375·9	369·5	371·7	6·24
300	368·0	55·85	382·1	376·4	378·4	6·59
410	373·3	53·77	386·0	381·0	382·8	6·94
500	376·8	52·27	388·6	384·0	385·7	7·21
600	379·3	51·06	390·4	386·2	387·8	7·43
680	381·9	50·61	392·6	388·5	390·1	7·55
820	385·0	49·93	395·2	391·4	393·0	7·71
1000	388·7	49·59	398·7	395·0	396·5	7·84
1150	390·8	49·36	400·6	397·0	398·5	7·91
1480	395·1	47·95	404·1	401·0	402·4	8·24
1890	397·9	48·31	406·9	403·7	405·1	8·23

Table 2. Beam parameters of CF_4.

P_0 (Torr)	u (ms^{-1})	α_s (ms^{-1})	v_m (ms^{-1})	$\langle v_{\parallel} \rangle$ (ms^{-1})	$\langle v_{\parallel}^2 \rangle^{1/2}$ (ms^{-1})	$S_{\parallel}$
100	437·9	84·49	465·2	457·9	457·6	5·18
220	452·3	68·44	468·4	462·5	465·0	6·61
300	455·7	65·33	470·5	465·0	467·2	6·98
420	460·8	59·90	472·1	468·6	470·5	7·69
620	467·2	54·97	476·5	473·6	475·2	8·50
800	471·1	51·24	478·7	476·7	478·0	9·20
1000	474·3	49·17	480·9	479·3	480·6	9·65

Table 3. Beam parameters of NH_3.

P_0 (Torr)	u (ms^{-1})	α_s (ms^{-1})	v_m (ms^{-1})	$\langle v_{\parallel} \rangle$ (ms^{-1})	$\langle v_{\parallel}^2 \rangle^{1/2}$ (ms^{-1})	$S_{\parallel}$
80	982·7	160·0	1017·5	1008·1	1014·2	6·14
110	1000·0	138·4	1025·0	1022·1	1026·5	7·25
150	1032·2	124·3	1045·0	1047·0	1050·6	8·31
180	1042·2	107·9	1048·4	1053·2	1056·1	9·66
240	1048·0	93·8	1053·0	1055·8	1058·1	11·17
320	1061·5	85·6	1064·3	1068·6	1070·1	12·40

Table 4. Beam parameters of CHF_3.

P_0 Torr)	u (ms^{-1})	α_s (ms^{-1})	v_m (ms^{-1})	$\langle v_\parallel \rangle$ (ms^{-1})	$\langle v_\parallel^2 \rangle^{1/2}$ (ms^{-1})	$S_\parallel$
80	475·80	90·37	504·30	492·50	496·60	5·27
120	486·20	81·83	508·60	499·70	502·98	5·94
155	491·50	75·33	509·80	502·90	505·70	6·53
200	498·40	72·60	514·90	508·90	511·40	6·87
260	501·60	69·30	516·20	511·02	513·30	7·24
320	505·70	65·20	518·10	514·10	516·10	7·76
420	510·20	62·97	521·40	517·90	519·80	8·10
520	513·20	61·05	523·30	520·40	522·10	8·40
650	518·10	59·50	527·30	524·80	526·40	8·71
820	522·70	57·60	530·70	528·80	530·30	9·10
1000	526·60	57·60	534·80	532·90	534·40	9·13
1200	530·90	57·90	539·00	537·10	538·70	9·18

Table 5. Beam parameters of SF_6–Ar.

% SF_6	P_0 (Torr)	u (ms^{-1})	α_s (ms^{-1})	T (K)	γ	$S_\parallel$
39	345	476·9	30·96	4·7	1·36	15·40
24	350	489·8	27·54	3·0	1·45	17·78
44	350	455·0	36·05	6·8	1·37	12·62
51	350	439·9	39·11	8·7	1·36	11·24
24	500	493·1	23·09	2·1	1·45	21·35
28	500	482·8	27·63	3·2	1·44	17·48
32	500	484·1	26·89	3·2	1·40	18·00
36	500	475·7	29·16	4·0	1·39	16·31
40	500	462·3	32·39	5·2	1·39	14·28

the nozzle exit, for different values of stagnation pressure (P_0). All the velocities except characteristic velocity, α_s increase with P_0. The values of $\langle v_\parallel \rangle$ and $\langle v_\parallel^2 \rangle^{1/2}$ determined from their analytical expressions differed from those determined by numerical integration of the corresponding equations by less than 0·03%. At a stagnation pressure of 100 torr, more than 30% of SF_6 molecules have been found to be within 5% of the most probable velocity of the beam, and for the other gases, the value is even higher. In table 5, we present thermodynamic parameters of SF_6–Ar beams.

3.2 *Beam intensities*

The relative intensities of the supersonic beams were determined by integrating the area under the time-of-flight profiles. Figure 5 shows the measured relative intensities of beams of the various gases as a function of the stagnation pressure, with skimmer located at 11·5 mm downstream from nozzle exit. The beam intensities initially increase with pressure, and then reach a plateau in the pressure range investigated, in contrast to the linear increase expected from isentropic considerations. The increase in intensity

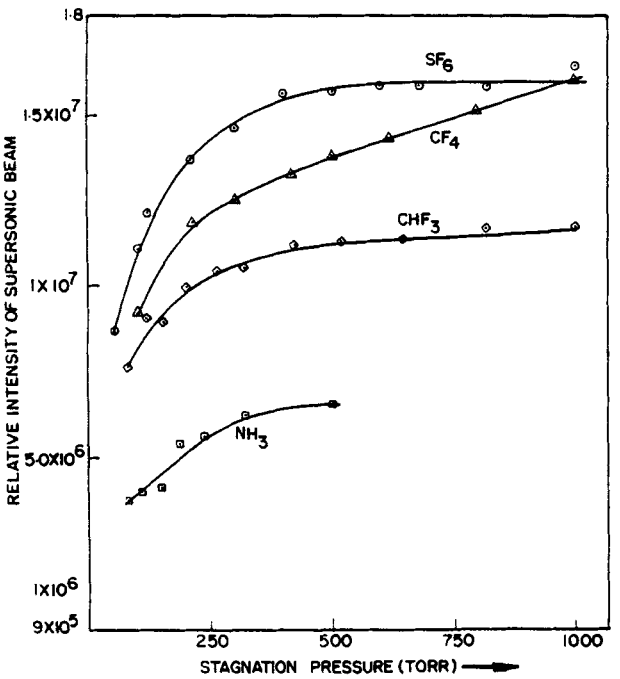

Figure 5. Relative beam intensities of the various molecules as a function of stagnation pressure.

with pressure beyond 400 torr of pressure is only nominal. It is believed that this behaviour is primarily due to skimmer interferences (Herschbach 1966).

3.3 *Specific heat ratio (γ) of polyatomic molecules during expansion*

The effective value of specific heat ratio, γ_{eff}, of a polyatomic gas in a supersonic jet depends on the expansion conditions, because the various degrees of freedom could be in a non-equilibrium state in the jet. The effective value of specific heat ratio for given expansion conditions is given by

$$\gamma_{\text{eff}} = \left[1 - \frac{1}{S_{\parallel}^2}\frac{T_0 - T_{\parallel}}{T_{\parallel}}\right]^{-1}. \tag{18}$$

The values of γ_{eff} for polyatomic gases thus determined are shown in figure 6 as a function of P_0. The specific heat ratio of SF_6, CF_4 and CHF_3 obtained from heat capacity data at 298 K are 1·12, 1·13 and 1·1 respectively (Stull *et al* 1969). Figure 6 shows that γ_{eff} in the jet is higher than the corresponding equilibrium value at stagnation temperature, and moreover, it decreases with P_0.

Hydrodynamic expansion of a gas results in a fast decrease in translational temperature as well as collision rate along the jet axis, which, in turn, progressively decrease the contribution of the internal degrees of freedom to the directed kinetic energy of the flow, and ultimately freeze this contribution somewhere along the flow axis, causing an increase in the effective value of the specific heat ratio, γ_{eff}.

Since the rotational spacing of SF_6 is quite small ($B_{SF_6} \simeq 0{\cdot}09111\,\text{cm}^{-1}$), its

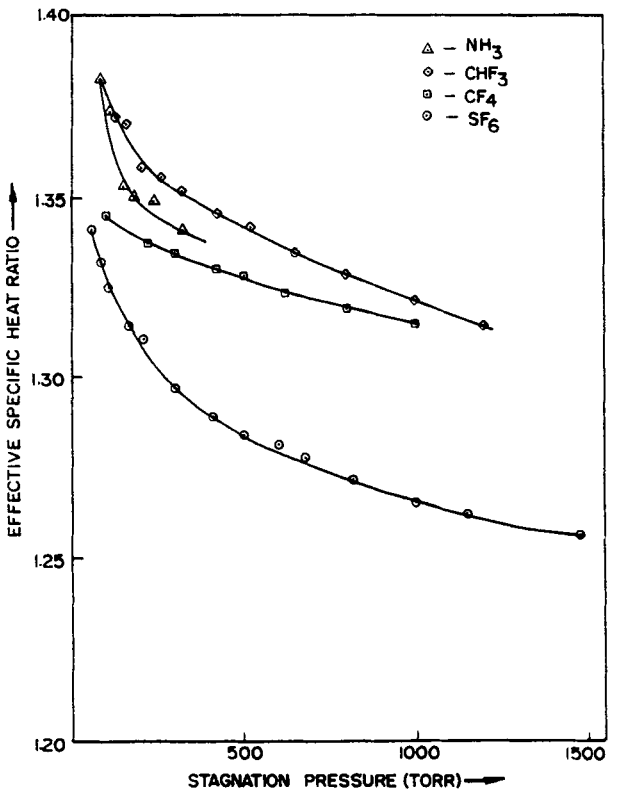

Figure 6. Effective specific heat ratios of the various molecules in a supersonic jet as a function of stagnation pressure.

rotational degrees of freedom are expected to be always in equilibration with the translational degree of freedom. The specific heat ratio of a polyatomic molecule, with rotational and translational degrees of freedom active and in equilibration, is 1·33. But, the specific heat ratio values determined at stagnation pressures less than 400 torr are higher than this value for all the gases except SF_6 (cf. figure 6), which indicates that even the rotational degrees of freedom partly lag behind the translational degrees of freedom. Thus, the higher value of specific heat ratio in the jet is due to lagging behind of the internal degrees of freedom, particularly, the vibrational degrees of freedom, during the expansion; vibrational relaxation is frozen within a few nozzle diameters at moderate P_0D values. Thus, at moderate P_0D values, the dominant factor contributing to the increase in γ_{eff} is the insufficient number of collisions for the relaxation of certain internal degrees of freedom during the transit time of the molecules through a certain region of the jet.

As the stagnation pressure increases, the total number of collisions experienced by a molecule would also increase. Consequently, the relaxation of the internal degrees of freedom will be more effective. Therefore, the decrease in specific heat ratio with P_0 is attributed to enhancement in the relaxation of the internal degrees of freedom. The higher values of effective specific heat ratio of CF_4 ($\nu_{min} = 437\,cm^{-1}$) as compared to that of SF_6 ($\nu_{min} = 347\,cm^{-1}$) indicates lower degree of internal relaxation in CF_4 than that in SF_6 during the expansion.

3.4 *Vibrational relaxation*

As mentioned in the previous section, the decrease in effective specific heat ratio of a polyatomic molecule in the jet with P_0 indicates vibrational relaxation. The extent of vibrational relaxation can be determined by measuring the vibrational temperature. In the present studies, vibrational temperature, T_{vib}, has been estimated from the energy balance equation (Coulter *et al* 1980; Anderson 1974)

$$4kT_0 + \int_0^{T_0} c_v(\text{vib})\mathrm{d}T = \frac{3}{2}kT_{\parallel} + kT_{\perp} + \frac{3}{2}kT_{rot} + \int_0^{T_{vib}} c_v(\text{vib})\mathrm{d}T + \frac{1}{2}mu^2 \tag{19}$$

where $T_{\parallel}$ and $T_{\perp}$ are the parallel and perpendicular translational temperatures respectively, T_{rot} is the rotational temperature and $c_v(\text{vib})$ is the vibrational contribution to the specific heat ratio at constant volume. Since time-of-flight data were obtained by skimming the jet at 11·5 mm ($x/D = 153$) downstream from the nozzle exist, we can assume $T_{\perp} = 0$. Since B_{SF_6} is very small, the rotational temperature can be taken to be equal to the parallel translational temperature. The vibrational heat capacity of SF_6 at constant volume, $c_v(\text{vib})$, in the temperature range 150 to 300 K is given by (Coulter *et al* 1980)

$$c_v(\text{vib}) = [0{\cdot}03552\,kT - 2{\cdot}629\,k]\,\text{J/molecule}. \tag{20}$$

Substitution of the value of c_v into (19) and integration result in a quadratic equation, the solution of which will give the value of vibrational temperature. Vibrational temperature of SF_6 thus obtained is shown in figure 7 as a function of the stagnation pressure.

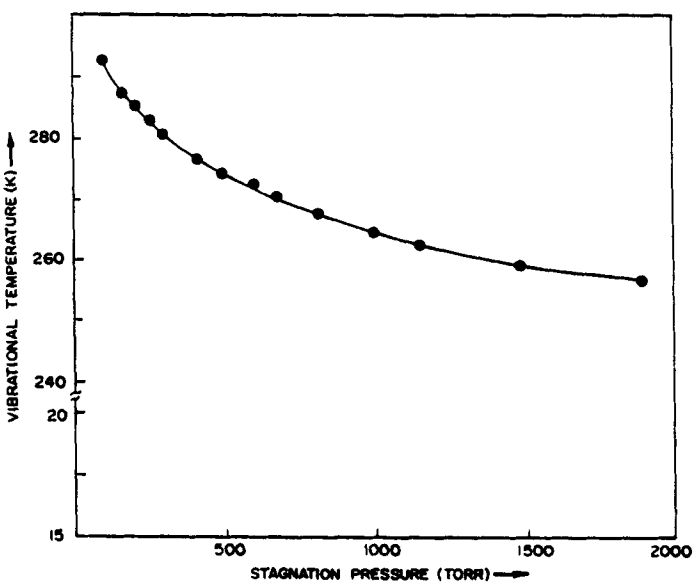

Figure 7. Vibrational temperature of SF_6 as a function of stagnation pressure.

3.5 *Collision effectiveness*

Collision effectiveness is an important parameter determining efficiency of a collision in achieving translational relaxation. It is, therefore, extremely useful to know this parameter for different gases. It can be determined from the measured terminal translational temperature as follows. The terminal translational temperature is given by

$$\frac{T_T}{T_0} = \left[1 + \frac{1}{2}(\gamma - 1)M_T^2\right]^{-1} \tag{21}$$

where the terminal Mach number, M_T, in a free-jet from a circular orifice or nozzle is (Bajaj and Chakraborti 1986)

$$M_T = F(\gamma)[K_{n_0}/\varepsilon]^{-(\gamma-1)/\gamma} \tag{22}$$

where $F(\gamma)$ is (Bajaj and Chakraborti 1986)

$$F(\gamma) = 2^{(3\gamma - 2/2\gamma)}\gamma\left[\{\pi\gamma(\gamma-1)\}^{(\gamma-1/\gamma)}\left\{\frac{1}{2}A(\gamma)^2(\gamma-1)^{\gamma+1}\right\}\right]^{-\frac{1}{4}}. \tag{23}$$

Substitution of M_T in (21), and subsequent rearrangement give

$$\varepsilon = \left[\frac{2}{\gamma-1}\{T_0/T_T - 1\}F(\gamma)^{-2}\right]^{(\gamma/2(\gamma-1)} K_{n_0}. \tag{24}$$

The values of $A(\gamma)$ required to calculate $F(\gamma)$ were determined by interpolation of the values given in literature (Anderson 1974), and hard-sphere collision cross-sections were used to calculate Knudsen number, K_{n_0}. The collision effectiveness was then determined by replacing T_T in (24) with the experimental translational temperature at $x/D = 11{\cdot}5$ mm, because there was no change in translational temperature after $x/D = 7{\cdot}0$ mm. The average value of collision effectivenesss of SF_6 ($d = 5{\cdot}51$ Å) in the pressure range 300–1500 torr has been found to be 0·1 whereas that of CF_4 ($d = 4{\cdot}7$ Å) in the pressure range 300–1000 torr is 0·15. These values are lower than that of Ar (Anderson and Fenn 1967). In polyatomic molecules, even if the fractional change in random velocity per collision is more, there will be constant flow of energy to the translational modes due to relaxation of the internal modes of the molecules, thus making the effective value of ε smaller than what it would have been for a $T - T$ transfer. Therefore, ε is now a measure of the overall relaxation efficiency of the molecule at given expansion conditions. The higher value of ε for CF_4 as compared to that for SF_6 could be due to lower degree of internal relaxation in CF_4 than that in SF_6 during the expansion.

4. Conclusion

Time-of-flight technique has been used to characterize supersonic beams of polyatomic molecules in terms of translational temperature, speed ratio, flow velocity, characteristic velocity, most probable velocity, average velocity and root mean square velocity. Collision effectiveness and effective specific heat ratio of polyatomic gases pertinent

to jet expansion have also been determined. The effective specific heat ratio in a supersonic jet is higher than that at the stagnation temperature, and is found to decrease with the stagnation pressure. The higher value of the specific heat ratio at moderate stagnation pressure has been attributed to insufficient number of collisions for the relaxation of internal degrees of freedom during the transit time of the molecule through a certain region of the jet. The decrease in effective specific heat ratio with pressure has been attributed to enhancement in the degree of vibrational relaxation. Vibrational temperature of SF_6 has been determined by using energy balance considerations.

References

Alcalay J A and Knuth E L 1969 *Rev. Sci. Instrum.* **40** 438

Amirav A and Even U 1980 *J. Appl. Phys.* **51** 1

Anderson J B and Fenn J B 1967 *Phys. Fluids* **8** 780

Anderson J B 1974 in *Molecular beam and low density gas dynamics*, (ed) P P Wegner (New York: Dekker) vol. 4 p. 31

Apatin V M, Dorozhkin L M, Makarov G N and Pleshkov G M 1980 *Appl. Phys.* **B29** 273

Bajaj P N and Chakraborti P K 1986 *Chem. Phys.* **104** 41

Bajaj P N, Talukdar R, Chakraborti P K and Kartha V B 1989 *J. Mol. Struct.* **194** 117

Brusdeylins G, Meyer H D, Toennies J P and Winkelman K 1976 *AIAA progress in astronautics and aeronautics* (New York: American Institute of Astronautics and Aeronautics)

Cardillo H J, Ching C S Y, Green F E and Becker G E 1978 *J. Vac. Sci. Technol.* **15** 423

Coulter D R, Grabiner F R, Casson L , Flynn G W and Bernstein R B 1980 *J. Chem. Phys.* **73** 281

Gough T E, Miller R E and Scoles G 1977 *Appl. Phys. Lett.* **30** 338

Hayes J M and Small G J 1983 *Anal. Chem.* **55** 565

Herschbach D R 1966 *Adv. Chem. Phys.* **10** 319

King D L and Herschbach D R 1973 *Faraday Discuss. Chem. Soc.* **55** 331

Levy D H 1980 *Annu. Rev. Phys. Chem.* **31** 197

Miller R E, Watts R O and Ding A 1984 *Chem. Phys.* **83** 155

Schulz P A, Subdo Aa S, Grant E R, Shen Y R and Lee Y T 1980 *J. Chem. Phys.* **72** 4985

Shea J A and Flygare W H 1982 *J. Chem. Phys.* **76** 4857

Snavely D L, Colson S D and Wiberg K B 1981 *J. Chem. Phys.* **74** 6975

Stolte S 1982 *Berg. Bunsenges. Phys. Chem.* **86** 413

Stull D R, Westerum Jr E F and Sinke G C 1969 *Chemical thermodynamics of organic compounds*, (New York: Wiley)

Travis D N, McGurk J C, McKeown D and Denning R G 1977 *Chem. Phys. Lett.* **45** 287

Valente E J and Bartell L S 1984 *J. Chem. Phys.* **80** 1458

Vallentini J J, Esherick P and Owyoung A 1980 *Chem. Phys. Lett.* **75** 590

Veeken K and Reuss J 1984 *Appl. Phys.* **B34** 149

Young W S 1973 *Rev. Sci. Instrum.* **44** 715